

N71-23102

**NASA TECHNICAL  
MEMORANDUM**

**NASA TM X-52991**

NASA TM X-52991

**CASE FILE  
COPY**

**ANALYSIS OF ROTATIONAL EFFECTS ON COMPRESSIBLE  
VISCOSUS FLOW ACROSS SHAFT FACE SEALS**

by John Zuk and Lawrence P. Ludwig

Lewis Research Center  
Cleveland, Ohio

TECHNICAL PAPER proposed for presentation at  
Annual Meeting of the American Society of  
Lubrication Engineers  
Boston, Massachusetts, May 3-6, 1971

ANALYSIS OF ROTATIONAL EFFECTS ON COMPRESSIBLE

VISCOUS FLOW ACROSS SHAFT FACE SEALS

by John Zuk and Lawrence P. Ludwig

National Aeronautics and Space Administration

Lewis Research Center

Cleveland, Ohio

ABSTRACT

The flow across a parallel sealing dam of the type that appears in noncontacting shaft face seals is analyzed for steady, laminar, subsonic, isothermal compressible flow with relative rotation of the sealing dam surfaces. Rotational effects on leakage rates, pressure profiles, and other physical quantities of interest are found. Conditions are given under which a hydrostatic analysis of the radial leakage flow is a valid approximation. The error in estimating the mass leakage by using the hydrostatic radial flow formula is given. Engineering formulas presented include mass leakage flow rate, pressure and velocity distributions, opening force and center of pressure. The physics of the flow are discussed.

NOMENCLATURE

A	cross-sectional area, in. <sup>2</sup>
a	speed of sound, ft/sec
$C_p$	specific heat at constant pressure, Btu/(1bm)( <sup>°</sup> R)
$C_v$	specific heat at constant volume, Btu/(1bm)( <sup>°</sup> R)
$D/Dt$	material derivative, $\partial/\partial t + u(\partial/\partial r) + (v/r)(\partial/\partial \theta) + w(\partial/\partial z)$
$E_i( )$	exponential integral function
F	sealing dam force, lbf
$\vec{F}$	body force vector

$h$  film thickness, nominal, in.

$K_1$  dimensionless parameter =  $-3R_2^2\Omega^2/5RT$

$L$  sealing dam width, in.

$$E(X) = \sum_{n=1}^{\infty} \frac{K_1^n (X^{2n} - 1)}{2^{n+1} n n!}$$

$M$  Mach number

$\dot{M}$  mass flow, lbm/min

$\dot{\Delta M}$  change in mass flow

$\dot{M}^*$  dimensionless mass flow,  $12\mu M R T / \pi h^3 P_2$

$m$  molecular weight of gas, lbm/lb-mole

$n$  an integer

$P$  static pressure, psi

$\Delta P$  pressure differential, psi

$P_{min}$  smaller pressure of two pressure boundary conditions, psi

$P^*$  dimensionless pressure,  $P/\rho_0 U^2$

$\tilde{P}^2$  dimensionless  $P^2$ ,  $P^2/P_2^2$

$R$  universal gas constant,  $1545.4 \text{ ft-lbf/(lb-mole)} ({}^{\circ}R)$ ;

$\bar{R}$  mean radius,  $(R_1 + R_2)/2$ , in.

$\Delta R$  sealing dam length,  $R_2 - R_1$ , in.

$R$  gas constant,  $R/m$ ,  $\text{ft-lbf/(lbm)} ({}^{\circ}R)$

$Re_h$  pressure flow Reynolds number in radial direction,  $\rho U_h / \mu$

$Re_r$  shear flow Reynolds number in circumferential direction,  $\rho \bar{R} \Omega h / \mu$

$Re^*$  modified Reynolds number,  $Re_h h / \Delta R$

$r$  radial direction coordinate

$r^*$	dimensionless radial coordinate, $r/\Delta R$
T	temperature, $^{\circ}\text{F}$
U	pressure flow reference velocity, ft/sec
u	velocity in r-direction or x-direction, ft/sec
$u^*$	dimensionless velocity, $u/U$
V	reference shear flow velocity, ft/sec
v	velocity in $\theta$ -direction, ft/sec
$v^*$	dimensionless velocity, $v/V$
w	velocity in y-direction, ft/sec
$w^*$	dimensionless velocity, $w/W_{\text{ref}}$
W	reference velocity across film thickness, $U(h/\Delta R)$ , ft/sec
$\tilde{X}$	transformed coordinate, $r/R_2$
$X_c$	center of pressure in radial or X-direction, in.
x	coordinate in pressure gradient direction
y	coordinate across film thickness
$y^*$	dimensionless coordinate, $y/h$
z	shear flow coordinate in Cartesian system
$\gamma$	specific-heat ratio, $C_p/C_v$
$\theta$	circumferential coordinate
$\lambda$	second viscosity coefficient or coefficient of bulk viscosity
$\mu$	absolute or dynamic viscosity, $(\text{lbf})(\text{sec})/\text{in.}^2$
$\nu$	kinematic viscosity, $\text{ft}^2/\text{sec}$
$\rho$	density, $(\text{lbf})(\text{sec}^2)/\text{in.}^4$
$\rho^*$	dimensionless density, $\rho/\rho_0$
$\Omega$	angular rotational velocity, rad/sec
$\vec{\nabla}$	Del operator, $(\partial/\partial r)\hat{i} + (1/r)(\partial/\partial \theta)\hat{j} + (\partial/\partial z)\hat{k}$

Subscripts:

av	average
h	based on film thickness
r	based on radius
0	reference
1	inner radius
2	outer radius

## INTRODUCTION

Some powerplants, such as advanced jet engines, exceed the operating limits of face contact seals (Refs. 1 and 2). As a result, noncontact face seals are becoming necessary. A noncontact face seal which is pressure (force) balanced is shown in Fig. 1. In this seal the leakage and pressure drop occur across a narrowly spaced sealing dam, and the axial force associated with this pressure drop is balanced by a predetermined hydrostatic closing force and a spring force. However, this configuration, with the sealing dam formed by parallel surfaces has an inherent problem: the force due to the pressure drop across the sealing dam is independent of film thickness; hence, there is no way of maintaining a preselected film thickness which will allow tolerable leakage and still have noncontact operation. Since the force is independent of film thickness, the design also lacks axial film stiffness for sufficient dynamic tracking of the stationary nosepiece with the rotating seal seat. The seal nosepiece must follow the seal seat surface under different operating conditions without surface contact or excessive increase in film thickness, which would yield high leakage. Some of these operating conditions are axial runout, misalignment, and thermal deformation

(coning and dishing).

A successful method of maintaining a preselected film thickness and achieving axial film stiffness is to add self-acting lift pads, such as shrouded Rayleigh step bearings, to the conventional face seal (1 and 2). This is illustrated in Fig. 2. The axial sealing dam force associated with the pressure drop across the sealing dam, and the lift pad force, are balanced by the hydrostatic and spring closing forces. The gas bearing has a desirable characteristic whereby the force increases with decreasing film thickness. If the seal is perturbed in such a way as to decrease the gap, the additional force generated by the lift pad will open the gap to the original equilibrium position. In a similar manner, if the gap becomes larger, the lift pad force decreases, and the closing force will cause the seal gap to return to the equilibrium position. Since a proper balance of the opening and closing forces must be found in order to determine a gap with a tolerable mass leakage, physical quantities of interest, such as pressure distribution and mass leakage, must be evaluated.

In this paper only the sealing dam portion of the seal will be analyzed. The classical viscous, isothermal, subsonic, compressible flow analysis for this problem is well known (e.g., see Gross, (3)). The pressure distribution and mass leakage have been calculated for the parallel film hydrostatic case. Reference (4) analyzed the parallel film hydrostatic case including the effects of fluid inertia, viscous friction and entrance losses. Subsonic and choked flow conditions can be predicted and analyzed for both laminar and turbulent flows. Results showed good agreement with experiment. The effects of rotation of the

much greater than  $h$ , the entrance region effects are neglected; hence, the convective inertia forces are neglected. This means that the seal is treated as operating entirely in the viscous region. This case is contrasted to the case where the gap size is large, as illustrated in Fig. 4(b) for a radial diffuser. 6) The fluid film is isothermal. This means that all heat generated in the film is conducted away through the walls. This is a standard assumption of lubrication theory. The validity of this assumption breaks down for cases of large thermal gradients in the sealing dam and when the frictional heating is high (e.g., small gap or high speed). However, thermal analysis of a gas film seal (2) shows that the sealing dam can be closely approximated by a constant temperature. The limit of the validity of isothermal duct flow analyses is that  $M < 1/\sqrt{\gamma}$  (6). 7) The entrance Mach number is close to zero. This means that there cannot be a large axial flow source on one surface impinging on the radial surface, as in a hydrostatic bearing (Fig. 4(c)). 8) The fluid velocity in the reservoir is considered to be negligible (stagnant), and thus its effects are neglected in this analysis. This model is, therefore, not valid for the radial step seal shown in Fig. 4(d) when radial velocities are significant.

#### Governing Equations

The analysis will be outlined briefly. Further details can be found in (7). The governing flow equations for a compressible fluid with constant viscosity in vector notation are (8)

Conservation of mass:

$$\frac{D\rho}{Dt} + \rho \vec{\nabla} \cdot \vec{V} = 0 \quad [1]$$

seal seat with respect to the seal nosepiece (sealing dam surfaces) on the radial pressure flow, however, have been neglected in these compressible flow analyses. Snapp (5) has analyzed the effects of rotation for the incompressible flow case.

This analysis was conducted 1) to investigate theoretically the effect of the relative rotation of the sealing faces on mass leakage, pressure and velocity distributions, net pressure opening force, and center of pressure (radial direction) for an isothermal, compressible, viscous flow with parallel sealing dam surfaces; 2) to determine under what conditions, if any, the hydrostatic radial flow analysis is sufficient for engineering accuracy.

#### ANALYSIS

##### Basic Model

The sealing dam model, as shown in Figs. 3 and 4(a), consists of two parallel, coaxial, circular rings in relative rotation at a constant speed separated by a very narrow gap. A pressure differential exists between the rings' inner and outer radii. The fluid velocities are small in both the inner-diameter cavity and outer-diameter cavity which bound the sealing dam.

The model formulation is based on the following physical conditions:

- 1) The fluid is homogeneous, compressible, viscous, and Newtonian.
- 2) The flow is steady and laminar (continuum flow regime), and the body forces are negligible.
- 3) The bulk modulus is ignored ( $\lambda = -2/3 \mu$ ).

This is Stokes idealization (3). This condition will be valid unless the gas is under high pressure, very dense (e.g., shock-wave structure), or rarefied.

- 4) The fluid behaves as a perfect gas.
- 5) Since  $\Delta R$  is

Conservation of momentum (Navier-Stokes equations):

$$\rho \frac{\vec{D}\vec{V}}{Dt} = -\vec{\nabla}P - \mu \vec{\nabla} \times (\vec{\nabla} \times \vec{V}) + \left(\frac{4}{3}\mu\right) \vec{\nabla}(\vec{\nabla} \cdot \vec{V}) + \vec{F} \quad [2]$$

Equation of state for an isothermal process:

$$P = P(\rho) \quad [3]$$

By using cylindrical coordinates (Fig. 3) and by applying the conditions assumed in the mathematical model, including the narrow gap approximation, the governing flow of a compressible fluid equations in dimensionless form reduce to

Conservation of mass

$$\frac{1}{r^*} \frac{\partial}{\partial r^*} (\rho^* r^* u^*) = 0 \quad [4]$$

Conservation of momentum

1) Radial direction

$$\rho^* u^* \frac{\partial u^*}{\partial r^*} - \left(\frac{V}{U}\right)^2 \frac{\rho^* v^*}{r^*} = -1 \frac{\partial P^*}{\partial r^*} + \frac{1}{Re^*} \frac{\partial^2 u^*}{\partial y^* 2} \quad [5]$$

2) Circumferential direction

$$\rho^* \left[ u^* \frac{\partial v^*}{\partial r^*} + w^* \frac{\partial v^*}{\partial y^*} + \frac{u^* v^*}{r^*} \right] = \frac{1}{Re^*} \frac{\partial^2 v^*}{\partial y^* 2} \quad [6]$$

3) Axial direction

$$\frac{\partial P^*}{\partial y^*} \approx 0, \quad \text{since} \quad \frac{\partial P^*}{\partial y^*} \sim 0 \left[ \left( \frac{h}{\Delta R} \right)^2 \right] \quad [7]$$

Equation of state

$$\frac{P^*}{\rho^*} = \text{constant} \quad [8]$$

Equations [4] to [8] have been nondimensionalized with the following variables:

$$r^* = \frac{r}{\Delta R}$$

$$P^* = \frac{P}{\rho_0 U^2}$$

$$w^* = \frac{w}{W}$$

$$y^* = \frac{y}{h}$$

$$\rho^* = \frac{\rho}{\rho_0}$$

$$Re_h^* = \frac{\rho_0 U h}{\mu}$$

$$u^* = \frac{u}{U}$$

$$v^* = \frac{v}{V}$$

$$Re^* = Re_h^* \left( \frac{h}{\Delta R} \right)$$

All the dimensionless terms with the exception of  $r^*$  are of unit magnitude ( $r^*$  is of greater than unit magnitude). By neglecting the entrance region and assuming  $Re^* \ll 1$ , the convective inertia forces are neglected. Hence the dimensionless radial momentum Eq. [5] becomes

$$-\left(\frac{V}{U}\right)^2 \rho^* \frac{v^*}{r^*} = -\frac{\partial P^*}{\partial r^*} + \frac{1}{Re_h^*} \left(\frac{\Delta R}{h}\right) \frac{\partial^2 u^*}{\partial y^*} \quad [9]$$

It is important to note that if  $V/U < 1/\sqrt{Re_h^*(h/\Delta R)}$ , the radial pressure flow can be treated as uncoupled from the rotational shear flow. This condition justifies the use of radial hydrostatic leakage flow equations for gas film seals whose sealing faces are in relative rotation. Again for  $Re^* \ll 1$  Eq. [6] becomes

$$\frac{\partial^2 v^*}{\partial y^*} = 0 \quad [10]$$

Now in dimensional form the equations to be solved are

Conservation of mass (from Eq. [4]):

$$\frac{\partial}{\partial r} (\rho r u) = 0 \quad [11]$$

(This form of the continuity equation is not used but is replaced by the integrated form, which is shown to be the conservation of mass flow in the radial direction.)

Radial momentum (from Eq. [5]):

$$-\frac{\rho v^2}{r} = -\frac{\partial p}{\partial r} + \mu \frac{\partial^2 u}{\partial y^2} \quad [12]$$

(The centripetal inertia term on the left side is ignored in the compressible Reynolds lubrication equation.)

Circumferential momentum (from Eq. [6]):

$$\frac{\partial^2 v}{\partial y^2} = 0 \quad [13]$$

Now the above set of equations will be solved. Equation [13] may be integrated directly. Applying the boundary conditions

$$v = 0 \quad \text{at} \quad y = 0 \quad v = r\Omega \quad \text{at} \quad y = h$$

yields

$$v = \frac{r\Omega y}{h} \quad [14]$$

Now Eq. [12] is solved by substituting for the circumferential velocity equation (Eq. [14]) and the equation of state (Eq. [8]). Since the circumferential and axial variations are shown to be negligible,  $P = P(r)$ , and Eq. [12] becomes

$$\frac{\partial^2 u}{\partial y^2} = \frac{1}{\mu} \frac{dp}{dr} - \frac{\rho_0 \Omega^2}{P_0 h^2 \mu} r y^2 p \quad [15]$$

Integrating Eq. [15] in the  $y$ -direction and applying boundary conditions

$$u = 0 \quad \text{at} \quad y = 0 \quad u = 0 \quad \text{at} \quad y = h$$

yields

$$u = \frac{1}{2\mu} \frac{dp}{dr} (y^2 - hy) - \frac{\rho_0 \Omega^2 r p}{12\mu P_0 h^2} (y^4 - h^3 y) \quad [16]$$

The mass flow at any radius is

$$\dot{M} = 2\pi r \rho \int_0^h u dy = -\frac{\pi h^3 \rho r}{6\mu} \frac{dp}{dr} + \frac{\pi \rho_0^2 h^3 \rho r^2 p}{20\mu P_0} \quad [17]$$

Substituting the perfect gas law (Eq. [8]) into Eq. [17] yields

$$\dot{M} = -\left(\frac{\pi h^3 \rho_0}{12\mu P_0}\right) r \frac{dp^2}{dr} + \left(\frac{\pi \rho_0^2 h^3}{20\mu P_0^2}\right) r^2 p^2 \quad [18]$$

or

$$\frac{dp^2}{dr} - \left(\frac{3}{5} \frac{\rho_0 \Omega^2}{P_0}\right) r p^2 = -\left(\frac{12\mu P_0 \dot{M}}{\pi \rho_0 h^3}\right) \frac{1}{r} \quad [19]$$

To facilitate the solution, transform Eq. [19] in the following manner:

Let

$$\tilde{P} = \frac{P}{P_2} \quad \tilde{x} = \frac{r}{R_2}$$

$$\dot{M}^* = \frac{-12\mu \dot{M} \Omega T}{\pi h^3 P_2^2} \quad K_1 = -\frac{3R_2^2 \Omega^2}{5 \Omega T}$$

Thus, Eq. [19] becomes

$$\tilde{x} \frac{d\tilde{P}^2}{d\tilde{x}} + K_1 \tilde{x}^2 \tilde{P}^2 = \dot{M}^* \quad [20]$$

The conservation of mass must be satisfied

$$\frac{d\dot{M}^*}{d\tilde{x}} = 0 \quad [21]$$

(which replaces the continuity Eq. [4]) or

$$\frac{d}{d\tilde{x}} \left( \tilde{x} \frac{d\tilde{P}^2}{d\tilde{x}} \right) + K_1 \frac{d}{d\tilde{x}} (\tilde{x}^2 \tilde{P}^2) = 0 \quad [22]$$

Equation [22] can be solved subject to the following boundary conditions:

$$\left. \begin{array}{l} \tilde{X} = \tilde{X}_1 = \frac{R_1}{R_2} \\ \tilde{P}^2 = \tilde{P}_1^2 \end{array} \right\} \text{at } r = R_1 \quad \left. \begin{array}{l} \tilde{X} = 1 \\ \tilde{P}^2 = \tilde{P}_2^2 = 1 \end{array} \right\} \text{at } r = R_2$$

Equation [22] is a first-order nonhomogeneous ordinary differential equation with variable coefficients and can be solved by using the classical integrating factor method of solving differential equations. Applying the boundary conditions yields the following mass flow equation in dimensional form:

$$\dot{M} = - \frac{\pi h^3 \left\{ \exp \left[ \frac{-K_1}{2} \left( \frac{R_1^2}{R_2^2} - 1 \right) \right] P_2^2 - P_1^2 \right\} \exp \left( \frac{K_1}{2} \frac{R_1^2}{R_2^2} \right)}{12 \mu \mathcal{R} T \int_{R_1/R_2}^1 \frac{\exp \left( \frac{K_1}{2} \tilde{X}^2 \right)}{\tilde{X}} d\tilde{X}} \quad [23]$$

The integral in Eq. [23] can be expressed in terms of exponential integral function (9). In this form Eq. [23] becomes

$$\dot{M} = \frac{-\pi h^3 \left\{ \exp \left[ \frac{-K_1}{2} \left( \frac{R_1^2}{R_2^2} - 1 \right) \right] P_2^2 - P_1^2 \right\} \exp \left( \frac{K_1}{2} \frac{R_1^2}{R_2^2} \right)}{6 \mu \mathcal{R} T \left[ E_i(1) - E_i \left( \frac{R_1}{R_2} \right) \right]} \quad [24]$$

The resulting squared pressure distribution has integrals which can also be written in terms of exponential integral functions. Hence

$$P^2 = - \frac{\frac{E_i(1) - E_i\left(\frac{r}{R_2}\right)}{E_i(1) - E_i\left(\frac{R_1}{R_2}\right)}}{\exp\left[\frac{-K_1\left(\frac{r^2}{R_2^2} - \frac{R_1^2}{R_2^2}\right)}{2}\right]} \left\{ \exp\left[\frac{-K_1\left(\frac{R_1^2}{R_2^2} - 1\right)}{2}\right] P_2^2 - P_1^2 \right\} \\ + \exp\left[-\frac{K_1}{2}\left(\frac{r^2}{R_2^2} - 1\right)\right] P_2^2 \quad [25]$$

The total force per unit width is found from

$$\frac{F}{L} = \int_0^{R_2 - R_1} (P - P_{\min}) dX \quad [26]$$

Also the center of pressure is found from

$$X_C = \frac{\int_0^{R_2 - R_1} (P - P_{\min}) X dX}{\frac{F}{L}} \quad [27]$$

where  $P_{\min}$  is the smaller pressure of the two pressure boundary conditions. The integrations in Eqs. [23] to [27] are performed numerically in (10). Additional equations of interest in designing gas film seals are also given in (10).

Equations [25] and [26] show that the opening force does not depend on film thickness. Thus there is no axial film stiffness for the parallel sealing dam surface case, and some auxiliary device, such as self-acting lift pads, must be used to obtain axial film stiffness (see Fig. 2).

#### Circumferential Shear Flow

Under the conditions of this analysis, which include many shaft face seal applications, the circumferential flow is the well known simple Couette shear flow. The circumferential velocity distribution

is then given by Eq. [14] which is

$$v = \frac{r\Omega y}{h} \quad [14]$$

The total power can be estimated by considering the viscous shear due to rotation only

$$\text{Power} = \frac{\mu R^2 \Omega^2 A}{h} \quad [28]$$

#### Analytical Expressions for Special Cases

Small Parameter,  $K_1$

For most practical seal problems, the value of the parameter  $-K_1/2$  is less than 1. In this case the exponential integrals of Eqs. [24] and [25] can be evaluated by integrating an infinite series expansion. Thus analytical expressions can be found for the pressure distribution and mass leakage. Now,

$$\int \frac{\exp\left[\frac{K_1 \tilde{X}^2}{2}\right]}{\tilde{X}} d\tilde{X} = \left[ \frac{1}{\tilde{X}} + \frac{K_1 \tilde{X}}{2} + \frac{K_1^2 \tilde{X}^3}{2^2 \cdot 2!} + \frac{K_1^3 \tilde{X}^5}{2^3 \cdot 3!} + \dots + \left( \frac{K_1}{2} \right)^n \frac{\tilde{X}^{2n-1}}{n!} + \dots \right] d\tilde{X} = \ln \tilde{X} + \mathcal{E}(\tilde{X}) + C \quad [29]$$

where

$$\mathcal{E}(\tilde{X}) = \sum_{n=1}^{\infty} \frac{K_1^n (\tilde{X}^{2n} - 1)}{2^{n+1} n n!} \quad [30]$$

Thus, the mass flow Eq. [23] becomes

$$\dot{M} = \frac{\pi h^3 \left\{ \exp \left[ -\frac{K_1}{2} \left( \frac{R_1^2}{R_2^2} - 1 \right) \right] P_2^2 - P_1^2 \right\} \exp \left( \frac{K_1}{2} \frac{R_1^2}{R_2^2} \right)}{12 \mu R T \left[ \ln \left( \frac{R_1}{R_2} \right) + \mathcal{E} \left( \frac{R_1}{R_2} \right) \right]} \quad [31]$$

The resulting squared pressure distribution equation becomes

$$P^2 = - \frac{\ln \frac{r}{R_2} + \mathcal{E} \left( \frac{r}{R_2} \right)}{\ln \frac{R_1}{R_2} + \mathcal{E} \left( \frac{R_1}{R_2} \right)} \exp \left[ - \frac{\frac{K_1}{2} \left( \frac{r^2}{R_2^2} - \frac{R_1^2}{R_2^2} \right)}{2} \right] \left\{ \exp \left[ - \frac{K_1}{2} \left( \frac{R_1^2}{R_2^2} - 1 \right) \right] P_2^2 - P_1^2 \right\} + \exp \left[ - \frac{K_1}{2} \left( \frac{r^2}{R_2^2} - 1 \right) \right] P_2^2 \quad [32]$$

No Rotation

For no rotation,  $K_1 = 0$ ; hence,  $\mathcal{E}(r/R_2) = 0$ , and after substituting the perfect gas relation Eq. [31] becomes

$$\dot{M} = \frac{\pi h^3 (P_2^2 - P_1^2)}{12 \mu R T \ln \frac{R_1}{R_2}} \quad [33]$$

and Eq. [32] becomes

$$\frac{P^2}{P_2^2} = 1 - \left( 1 - \frac{P_1^2}{P_2^2} \right) \frac{\ln \frac{r}{R_2}}{\ln \frac{R_1}{R_2}} \quad [34]$$

Equations [33] and [34] are reducible to the form found in (3). In many gas film sealing dams  $\Delta R$  is much less than  $R_1$ . For this case

$$\ln \frac{R_1}{R_2} \approx - \frac{\Delta R}{R_1}$$

Eq. [33] becomes

$$\dot{M} = \frac{\pi R_1 h^3 (P_1^2 - P_2^2)}{12\mu \bar{R}T (R_2 - R_1)} \quad [35]$$

and Eq. [34] becomes

$$\frac{P_2^2}{P_1^2} = 1 - \left(1 - \frac{P_1^2}{P_2^2}\right) \frac{(r - R_2)}{R_2 - R_1} \left(\frac{R_1}{R_2}\right) \quad [36]$$

This is reducible to the form of the narrow slot leakage equation; thus, hydrostatic radial flow can be approximated with a narrow slot (plane flow) analysis with small error if  $(R_2 - R_1) \ll R_1$ .

For no rotation Eq. [27] can be readily integrated which results in

$$\frac{F}{L} = \frac{2P_1(R_2 - R_1) \left[ 1 - \left(\frac{P_2}{P_1}\right)^3 \right]}{3 \left[ 1 - \left(\frac{P_2}{P_1}\right)^2 \right]} - P_{\min}(R_2 - R_1) \quad [37]$$

The center of pressure can also be readily found from Eq. [28] which yields

$$x_c = \frac{L(R_2 - R_1)^2}{F} \left\{ \frac{P_1 \left[ \frac{2}{5} \left(\frac{P_2}{P_1}\right)^5 - \frac{2}{3} \left(\frac{P_2}{P_1}\right)^3 + \frac{4}{15} \right]}{\left[ 1 - \left(\frac{P_2}{P_1}\right)^2 \right]^2} - \frac{P_{\min}}{2} \right\} \quad [38]$$

#### Error in Estimating Mass Leakage by Hydrostatic Radial-Flow Formula

A formula will now be found to give the error that occurs in using the hydrostatic radial flow mass leakage equation when there is relative rotation of the sealing dam surfaces. Defining

$$\frac{\dot{M}}{\dot{M}_{\text{static}}} = \frac{\text{Eq. [31]} - \text{Eq. [33]}}{\text{Eq. [33]}}$$

and simplifying by applying conditions present in most sealing dams, namely, that

1) For  $|K_1/2| \ll 1$ ,

$$\exp\left(\frac{K_1}{2}\right) \approx 1 + \frac{K_1}{2}$$

and

$$\exp\left(\frac{K_1 R_1^2}{2R_2^2}\right) \approx 1 + \frac{K_1 R_1^2}{2R_2^2}$$

2) For  $R_1 \gg R_2 - R_1$ ,

$$\ln \frac{R_2}{R_1} \approx - \frac{\Delta R}{R_1}$$

$$3) \mathcal{L}(R_1/R_2) \approx K_1/4(R_1^2/R_2^2 - 1)$$

The above expression yields:

$$\frac{\dot{M}}{\dot{M}_{\text{static}}} = \frac{\Delta R \left[ 1 - \frac{P_1^2}{P_2^2} - \frac{3R_2^2\Omega^2}{5\mathcal{R}T} \left( 1 - \frac{P_1^2}{P_2^2} \frac{R_1^2}{R_2^2} \right) \right]}{R_1 \left( 1 - \frac{P_1^2}{P_2^2} \right) \left[ \frac{\Delta R}{R_1} + \frac{3R_2^2\Omega^2}{5\mathcal{R}T} \left( \frac{R_1^2}{R_2^2} - 1 \right) \right]} - 1 \quad [39]$$

#### DISCUSSION

##### Rotational Effects on Seal Leakage

For laminar flow across an isothermal compressible flow sealing dam, the change in mass leakage due to relative surface rotation would appear to be important when the surface speed is very high. Such an example, is a proposed space power generator (11) which requires small pressure

differential, low leakage seals at high rotational speeds (36 000 rpm). Figure 5 shows the effect of rotation on radial mass leakage for a proposed space power compressor seal. Both internally and externally pressurized modes are compared with the hydrostatic flow analysis. The film thickness varies from 0.1 mil to 0.3 mil which are practical operating gaps. The sealed fluid is a helium-xenon mixture. The operating conditions are: sealed pressure, 32 psia; ambient pressure, 31.5 psia; sealed gas temperature, 330° F; inner radius, 3.90 in.; outer radius, 4.00 in. The radii used in this example are larger than in (11). From Fig. 5, the hydrostatic analysis predicts about a 42% higher leakage than the rotational analysis when the seal operates in the externally pressurized mode. On the other hand, for the internally pressurized mode the rotational analysis shows that leakage is about 27% higher than predicted by the hydrostatic analysis. Rotational effects would be expected to be important for this case since the parameter  $V/U > 1/\sqrt{Re^*}$  ( $V/U = 310$ ,  $Re^{*-1/2} = 10$ ).

The approximate formula given by Eq. [39] can be used to determine whether rotation is important in radial mass leakage calculations. If rotational effects are shown not to be important, the simpler hydrostatic flow formulas can be used. Figure 6 illustrates that there is excellent agreement between the approximate formula (Eq. [39]), which includes only the first term of the convergent series, and the full solution using a computer program (10); radius ratios of 0.80 and 0.99 are shown for values of the parameter,  $-K_1/2 = 6 \times 10^{-6}$ . The approximate formula (Eq. [39]) predicts a 27% decrease in mass leakage due to rotation for the externally pressurized mode of the compressor seal example.

Even though rotation has a substantial effect on mass leakage, the pressure distribution is affected very little. The opening force changes by less than 1/2% and there was virtually no change in the center of pressure. Hence in this case the seal pressure balance is not affected by rotation.

The relative surface rotation appears to be negligible for many cases where the radial pressure differential is large, the gap is small, and the rotational speed is moderate. Such a case is evaluated in the appendix. This contrasts with the case for a liquid medium (incompressible fluid), where the centrifugal force in laminar radial flow can have a substantial effect because of the higher density. For example, water at room temperature is about three orders of magnitude more dense than air. The comparable incompressible viscous flow analysis (5) yields the following approximate formula.

$$\frac{\Delta M}{\dot{M}_{\text{static}}} = \frac{3\rho\Omega^2(R_2^2 - R_1^2)}{20(P_1 - P_2)} \quad [40]$$

If a very small pressure differential exists across the sealing dam, the rotational effects on the radial flow are important even for moderate speeds. An example of such a case is also given in the appendix.

The rotational flow is always important for determining the power loss (due to viscous shearing) and for determining the transition to turbulent flow. The rotational flow component of the velocity may be responsible for the flow becoming turbulent in the circumferential direction (shear flow direction), which will mean the entire flow field (radial pressure flow) will be turbulent.

Figure 7 illustrates a simplified envelope of possible sealing dam flow regimes, showing the region in which this analysis is valid. For the hydrostatic case, the viscous flow analysis presented is valid for  $Re_h(h/\Delta R) < 1$ . The parameter governing the flow regime for radial flow in most seal problems was found to be the Mach number rather than the pressure flow Reynolds number. This is true for very small gaps since calculations of (4) indicate that the flow can become choked in the radial direction before the transition (laminar to turbulent) pressure-flow Reynolds number is reached. Choking of the flow, of course, will occur when  $M = 1$ . The limit for this analysis to be valid is  $M < 1/\sqrt{\gamma}$ ; beyond this, the isothermal assumption no longer holds. (This is shown in (4). Reference (4) further shows that the adiabatic assumption is valid to  $M = 1$ .)

For radial pressure flow only, transition to turbulent flow will occur by Tollmien-Schlichting waves. The minimum transition Reynolds number  $Re_{2h}$  (based on an average velocity and hydraulic diameter) will be between 2300 and 6000; that is, between the minimum transition Reynolds number for fully developed pipe flow and what appears to be the theoretical minimum transition Reynolds number for plane Poiseuille flow (12) in infinitesimal disturbance hydrodynamic stability theory. The radial flow situation of the sealing dam approximates plane Poiseuille flow because the aspect ratio used in the hydraulic diameter calculation is the same.

For the case of only circumferential shear flow with no imposed radial pressure gradient, the flow will remain laminar until a critical rotational Reynolds number is exceeded; then the flow will become turbu-

lent. For this narrow gap sealing dam analysis ( $\Delta R \gg h$ ), the critical rotational Reynolds number for transition appears to be simple Couette flow transition Reynolds number. Thus,  $Re_r = \bar{R}\Omega h/v \approx 1900$  for transition (13); the smaller the gap, the longer transition speed is delayed. Thus, the wall has a stabilizing effect on the flow, and this should be considered in selecting the design gap (e.g., for a 1-ft-diam seal operating at room temperature, the transition speed would be 71 500 rpm for a 1-mil gap, but would be 179 000 rpm for a 0.4-mil gap).

When there is both circumferential shear flow and radial pressure flow present, the net flow is a spiral flow. To the authors' knowledge the transition from laminar to turbulent flow for this case has not been investigated.

Most flow regime transitions have been experimentally observed for incompressible flow between a disk and a confined housing, but there is reason to believe that transition will also occur for a compressible fluid in this range of Reynolds number. Theodorsen and Regier (14) conducted an experimental investigation on a rotating disk in an infinite compressible fluid medium and found that laminar-turbulent transition and drag are independent of Mach number. The highest transition Reynolds number  $(R_2^2 \Omega / v)$  was  $3 \times 10^5$  for the most highly polished disk. However, experimental work is needed to find the transition Reynolds number for compressible flow between two disks separated by a very narrow gap in relative rotation which is representative of gas film seal operation.

In this analysis, which is valid for a modified Reynolds number,  $Re_h (h/\Delta R) \ll 1$ , the circumferential velocity  $v$  can be found independently of the radial velocity  $u$  (i.e.,  $v$  does not depend on  $u$ , but

$u$  depends on  $v$  (see Eq. [13]). The radial velocity  $u$  is affected by the rotation through the centrifugal force component in the radial direction (see Eq. [12]). In a higher-order analysis, when  $Re_h(h/\Delta R)$  is no longer small, the fluid velocity component in the circumferential direction will depend on the radial pressure flow, which will, in turn, depend on the rotating flow velocity component.

The region where the radial and the tangential flow are coupled involves the solution of two simultaneous nonlinear partial differential equations and is beyond the scope of this analysis. This more complex formulation would be necessary for a stability analysis and for a more detailed examination of the flow field. In turbulent flow, of course, both the circumferential and radial flow velocity components depend on each other. However, the simplified analysis presented herein is representative of many shaft face seal applications.

In general leakage changes due to rotation must be considered with respect to other influences. Examples of other effects which under practical conditions may be of the same order or even more important are seal face deformations, surface wobbling, misalignment, and eccentricity.

#### Rotational Effects on Pressure and Velocity Profiles

The pressure distribution in the radial direction was found from Eq. [25]. The internally pressurized case is shown plotted in Fig. 8(a) for  $-K_1/2 = 0.02$ . Also shown in Fig. 8(a) is the hydrostatic radial pressure distribution, which was found from Eq. [25] with  $\Omega = 0$ . Note the sealing dam force is slightly greater for rotation. The radial pressure distribution for the externally pressurized case is shown in

Fig. 8(b). Here the sealing dam force is slightly less than for the hydrostatic case. As previously discussed, these pressure distributions are only slightly different than the hydrostatic case. Hence for most practical purposes the pressure balance is unaffected.

The radial velocity profiles for both internally and externally pressurized cases were found for  $R_1/R_2 = 0.99$ ,  $P_1/P_2 = 1.2$ , and  $-K_1/2 = 0.02$  and are shown in Figs. 9(a) and (b). These radial velocity profiles were obtained from Eq. [16]. Also shown are the hydrostatic and centrifugal force velocity components. As expected, the centrifugal force component is effective in reducing the leakage in the externally pressurized case whereas the opposite occurs in the internally pressurized case. The maximum velocity does not occur at the midgap position for the centrifugal force velocity component as it does for the hydrostatic component.

The shear flow (circumferential direction) velocity profile is the classical simple Couette flow profile.

#### SUMMARY OF RESULTS

The flow across a parallel sealing dam is analyzed for steady, laminar, subsonic, isothermal compressible flow with rotation. The assumed conditions are representative of many shaft face seal applications. The analysis considered the effect of relative seal face rotation on mass leakage, pressure distribution, velocity distribution, and net pressure force; the hydrostatic case was used for comparison. The following pertinent results were obtained:

1. Rotation has significant effects on seal leakage flow at high speeds. (The seal example analyzed has a 42% decrease in calculated

leakage for an externally pressurized sealing mode.) The seal pressure balance, however, appears to be substantially unaffected by rotation.

2. When the radial pressure differential is very small, rotational effects are also important at moderate speeds. (The seal example analyzed has a 17-percent increase in calculated leakage for a 0.2-psi pressure differential at a moderate speed.)

3. A hydrostatic analysis of the radial pressure flow is a good approximation of the rotating seal under the condition that the ratio of the reference radial pressure flow velocity to reference rotational velocity is greater than the square root of the modified Reynolds number.

4. The error in estimating the mass leakage by using the hydrostatic radial flow formula was analyzed, and a pertinent error analysis equation is given.

5. The region of validity of the analysis was defined as follows:

a. The analysis is valid until transition of the circumferential shear flow to turbulence.

b. The analysis is valid until the radial pressure flow approaches a Mach number of  $1/\sqrt{\gamma}$ , where  $\gamma$  is the ratio of specific heats, or until the radial pressure flow becomes turbulent.

6. The circumferential shear flow is important in that at high rotative speeds it can cause the flow field to become turbulent.

## REFERENCES

- (1) Ludwig, L. P., Zuk, J., and Johnson, R. L., "Use of the Computer in Design of Gas Turbine Mainshaft Seals for Operation to 500 ft/sec (122 m/sec)," Illinois Institute of Technology and Fluid Power Society, National Conference on Fluid Power (Chicago), 1970.
- (2) Povinelli, V. P., and McKibbin, A. H., "Development of Mainshaft Seals for Advanced Air Breathing Propulsion Systems, Phase II. Rep.," NASA Contractor Report 72737, June 1970.
- (3) Gross, W. A., "Gas Film Lubrication," Wiley, N.Y., 1962.
- (4) Zuk, J., Ludwig, L. P., and Johnson, R. L., "Compressible Flow Across Shaft Face Seals," NASA TM X-52959, April, 1971.
- (5) Snapp, R. B., "Theoretical Analysis of Face-Type Seals with Varying Radial Face Profiles," ASME Paper 64-WA/Lub-6, 1964.
- (6) Shapiro, A. H., "The Dynamics and Thermodynamics of Compressible Fluid Flow." Vol. I, Ronald Press Co., N.Y., 1953.
- (7) Zuk, J., and Ludwig, L. P., "Investigation of Isothermal, Compressible Flow Across a Rotating Sealing Dam. I - Analysis," NASA TN D-5344, Sept. 1969.
- (8) Hughes, W. F., and Gaylord, E. W., "Outline of Theory and Problems of Basic Equations of Engineering Science," Schaum Publ. Co., 1964.
- (9) Abramowitz, M., and Stegun, I. A., eds., "Handbook of Mathematical Functions with Formulas, Graphs, and Mathematical Tables," Applied Mathematics Series 55, National Bureau of Standards, 1964.
- (10) Zuk, J., Smith, Patricia J., and Ludwig, L. P., "Investigation of Isothermal, Compressible Flow Across a Rotating Sealing Dam. II - Computer Program," NASA TN D-5345, Sept. 1969.

- (11) Heath, B. B., and Luther, R. A., "The Design and Fabrication of the Brayton Rotating Unit Operating on Roller Element Bearings (BRU-R)," NASA Contractor Report 72642, Sept. 1969.
- (12) Nachtsheim, Philip R., "An Initial Value Method for the Numerical Treatment of the Orr-Sommerfeld Equation for the Case of Plane Poiseuille Flow, NASA TN D-2414, Aug. 1964.
- (13) Hinze, J. O., "Turbulence; An Introduction to Its Mechanism and Theory," McGraw-Hill, N.Y., 1959, p. 67.
- (14) Theodorsen, Theodore, and Regier, Arthur, "Experiments on Drag of Revolving Disk, Cylinders, and Streamline Rods at High Speeds, NACA TR 793, 1944.

APPENDIX - EXAMINATION OF CENTRIFUGAL FORCE EFFECT

(ROTATION) ON RADIAL AIRFLOW

Consider the following case. Let  $v = 2 \times 10^{-4}$  ft<sup>2</sup>/sec,  $T = 500^{\circ}$  R,  $\bar{R} = 1/2$  foot,  $\mathcal{Q} = 2 \times 10^3$  ft<sup>2</sup>/sec<sup>2</sup>- $^{\circ}$ R,  $N = 2300$  rpm (this can be considered a moderate speed), and  $h = 0.001$  inch. Hence,  $Re_r \approx 25$ , much less than the critical transition Reynolds number for simple Couette flow, which is about 1900. Since  $|K_1/2| \approx 4 \times 10^{-3}$ , Eq. [39] can be used to find the change in mass leakage caused by rotation.

Case I - Very Small Pressure Differential

When

$$\left. \begin{array}{l} P_1 = 100.2 \text{ psia}, R_1 = 5.70 \text{ in.} \\ P_2 = 100 \text{ psia}, R_2 = 6.30 \text{ in.} \end{array} \right\} \text{ at } \bar{R} = 1/2 \text{ ft}$$

Eq. [39] yields  $\dot{M}/\dot{M}_{\text{static}} \approx 17$  percent.

Hence, rotation also has a substantial effect on mass leakage when a very small pressure differential exists. In this example, the radial flow Mach number is very small, and the incompressible formula (Eq. [40]) predicts about a 25-percent change.

Case II - Moderate Pressure Differential

When

$$P_1 = 100 \text{ psia}, R_1 = 5.70 \text{ in.}$$

$$P_2 = 150 \text{ psia}, R_2 = 6.30 \text{ in.}$$

Eq. [39] yields

$$\frac{\dot{M}}{\dot{M}_{\text{static}}} \approx -0.1 \text{ percent}$$

Thus, the above example illustrates that centrifugal force usually does not have an appreciable effect on air mass leakage for moderate and large pressure ratios and moderate rotational speeds.

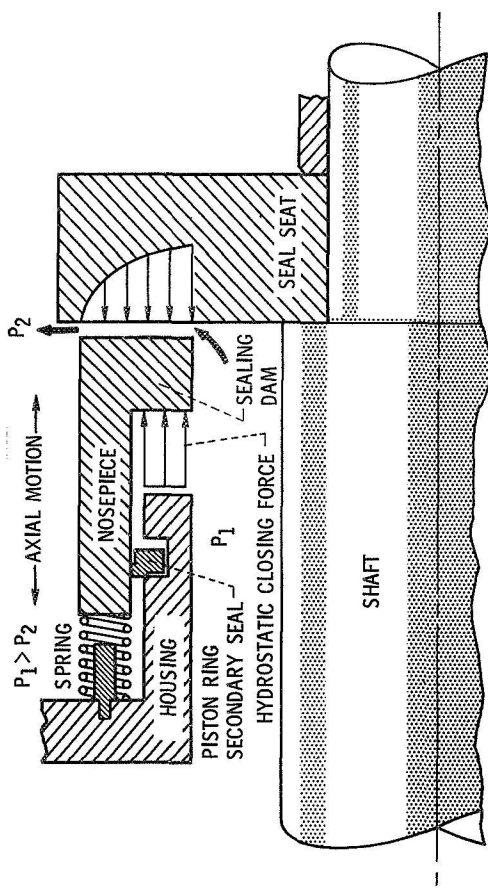


Figure 1. - Schematic of pressure balanced face seal, no axial film stiffness for parallel sealing surfaces.

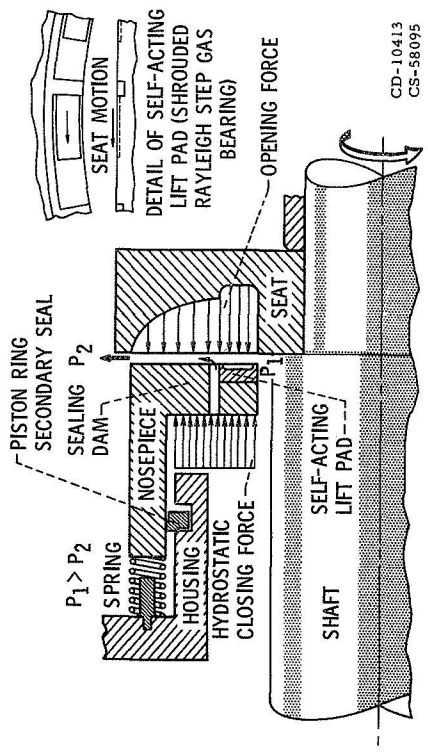


Figure 2. - Schematic of a pressure balanced face seal with self-acting lift pads added to obtain axial film stiffness.

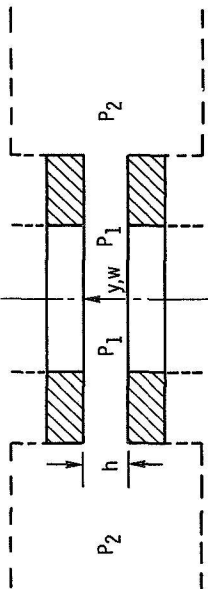
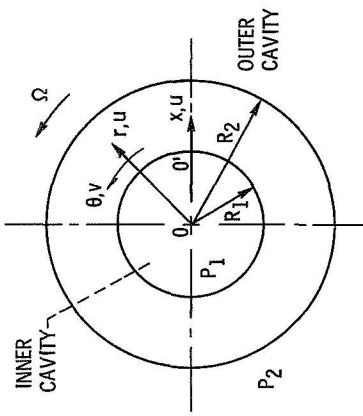
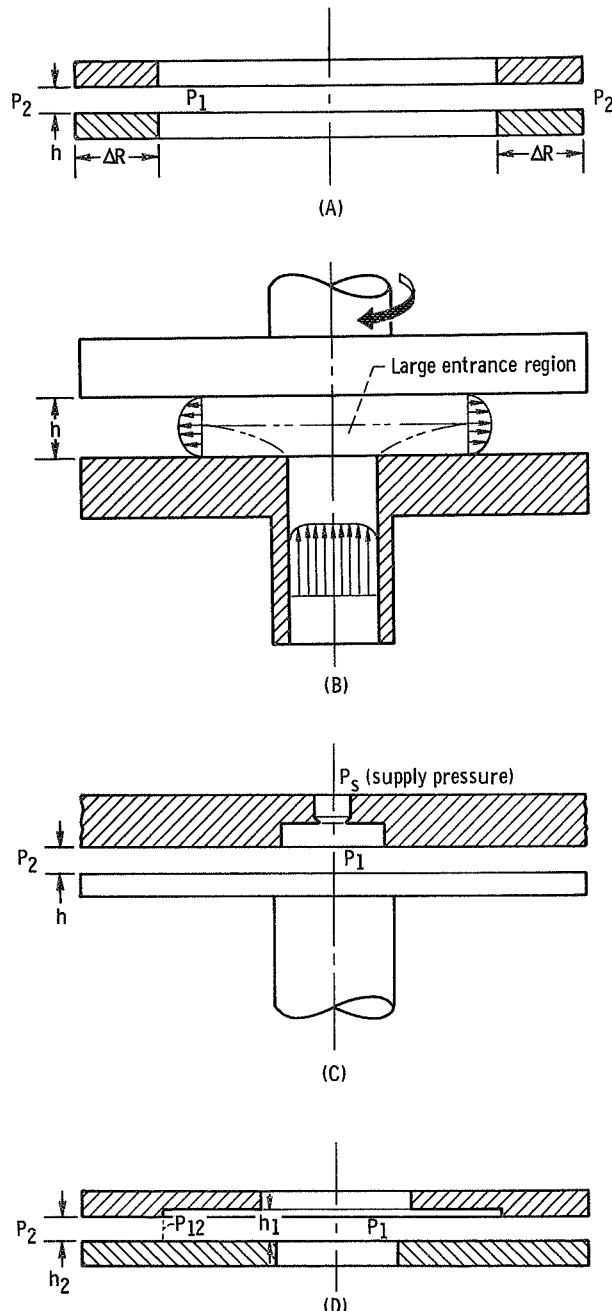


Figure 3. - Model of sealing dam.



(A) SEALING DAM MODEL USED IN ANALYSIS. MODEL CHARACTERISTICS:  
NO AXIAL FLOW; NARROW GAP,  $h \ll \Delta R$ .

(B) RADIAL DIFFUSER MODEL. MODEL DOES NOT CONFORM TO MODEL OF FIGURE 4(A) WHEN LARGE AXIAL FLOW RATES EXIST AND/OR  $\Delta R \sim \theta(h)$ .

(C) HYDROSTATIC OR EXTERNALLY PRESSURIZED THRUST BEARING MODEL.  
MODEL DOES NOT CONFORM TO MODEL OF FIGURE 4(A) WHEN SIGNIFICANT AXIAL FLOW THROUGH AN ORIFICE EXISTS.

(D) RADIAL STEP SEAL MODEL. MODEL OF FIGURE 4(A) IS VALID WHEN  $h_1 \gg h_2$  (THEN  $P_{12} \approx P_1$ ) AND INNER CAVITY VELOCITY IS NOT SIGNIFICANT.

Figure 4. - Various seal and bearing models illustrating conditions of analysis validity.

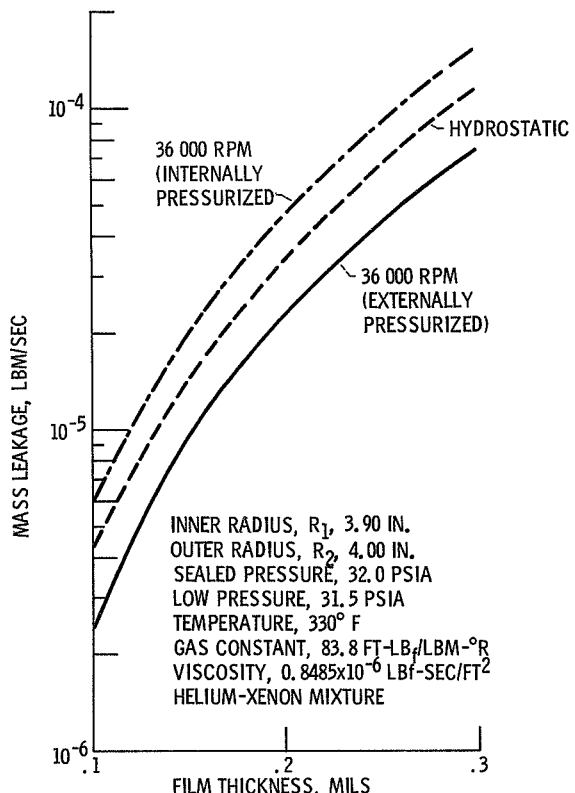


Figure 5. - Effect of rotation on mass leakage for a proposed space power compressor seal (11) for both internally and externally pressurized modes of operation.

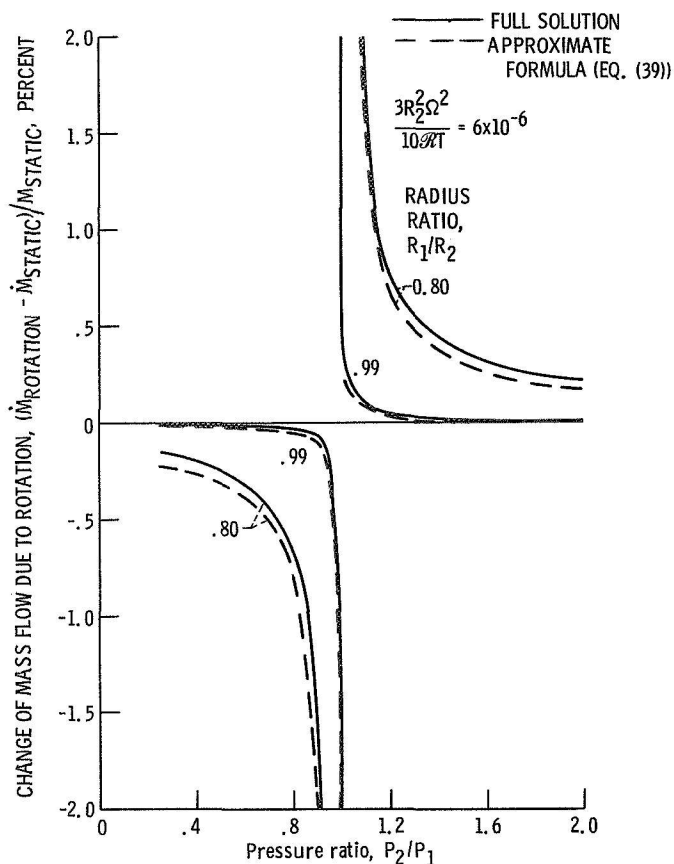


Figure 6. - Change of mass flow due to rotation as function of pressure ratio. Comparison of numerical solution with approximate formula.

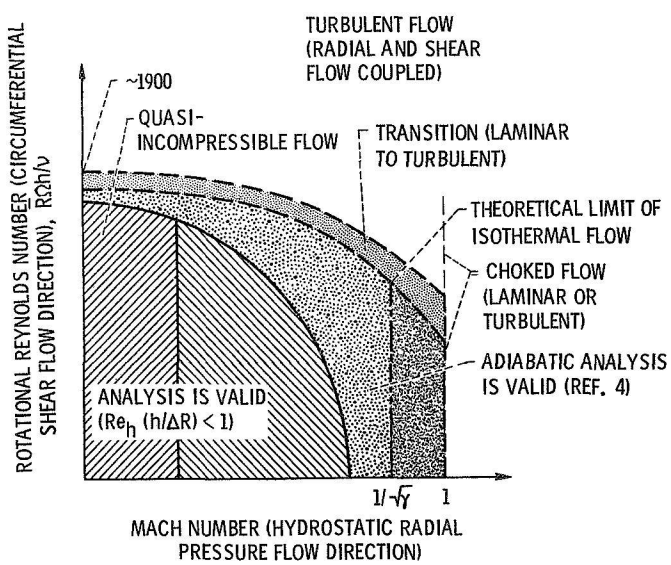


Figure 7. - Envelope of possible sealing dam flow regimes, illustrating region of analysis validity.

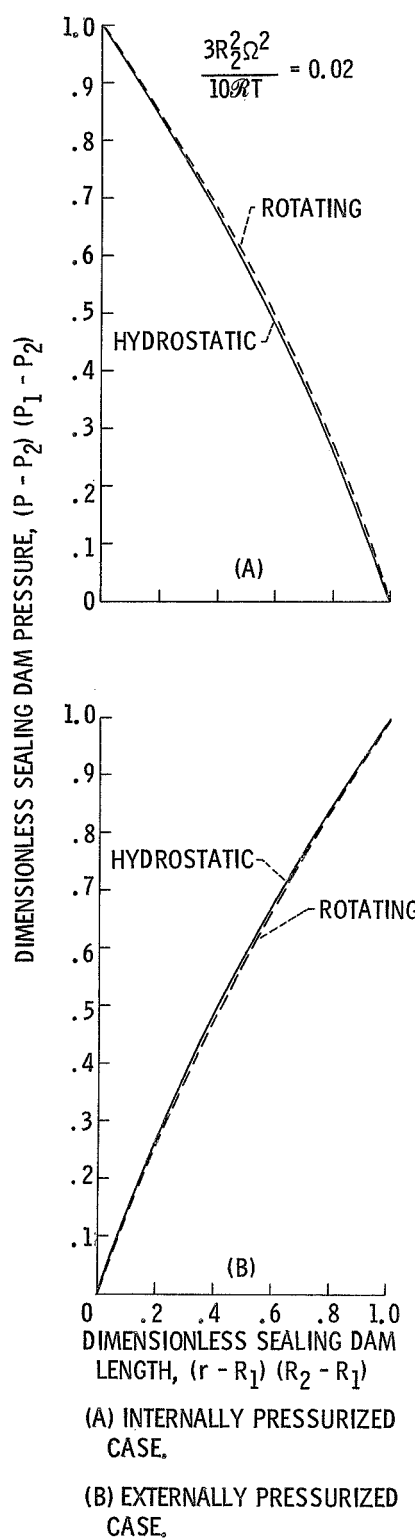


Figure 8. - Effect of rotation on radial pressure distribution.

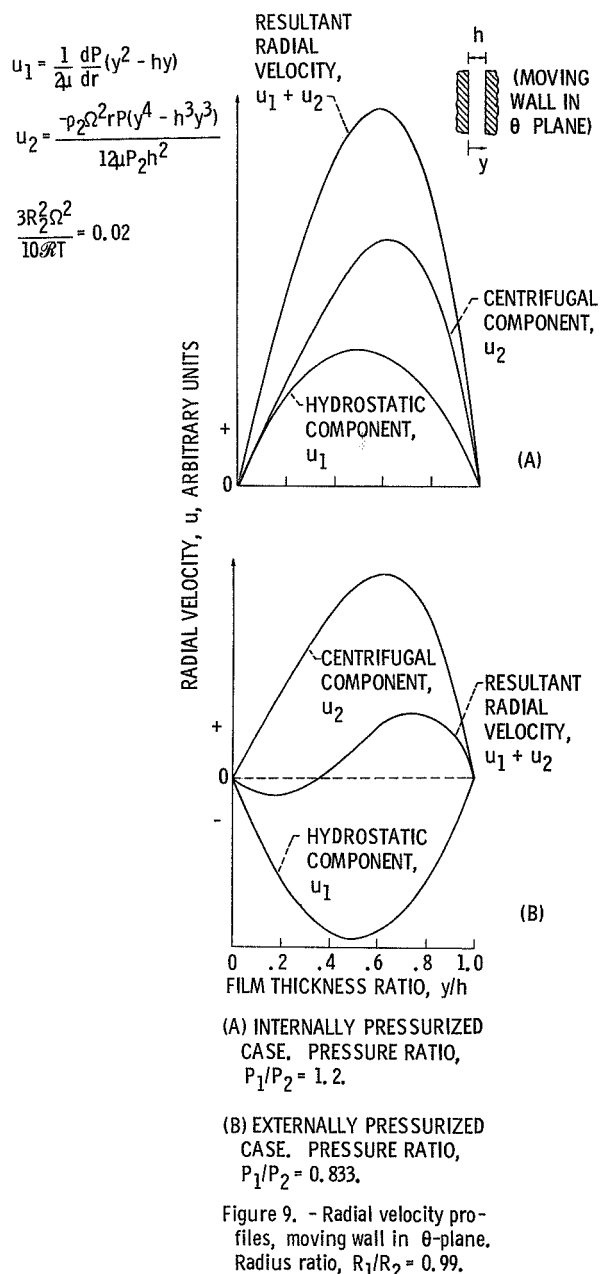


Figure 9. - Radial velocity profiles, moving wall in  $\theta$ -plane.  
Radius ratio,  $R_1/R_2 = 0.99$ .